Chemistry–A European Journal

Supporting Information

A Symmetrically π-Expanded Carbazole Incorporating Fluoranthene Moieties

Alexander Vogel, Till Schreyer, John Bergner, Frank Rominger, Thomas Oeser, and Milan Kivala*

Table of Contents

1 General Methods and Instrumentation

Cyclic voltammetry was performed on a computer-controlled BASi Cell Stand instrument under nitrogen atmosphere using a standard three-electrode assembly connected to a potentiostat and at a scan rate of 100 mVs^{-1}. The working electrode was a glassy carbon disk electrode (3.0 mm diameter), a platinum wire was used as auxiliary electrode and the quasi-reference electrode was an Ag/AgCl (3 M NaCl) electrode. The samples were measured in 0.1M electrolyte solutions of *n*-Bu_4NPF_6 (used without further purification) in anhydrous CH_2Cl_2 and were purged with nitrogen for 20 min prior to analysis. Each measurement was calibrated with an internal standard (ferrocene/ferrocenium (Fc/Fc^+)).

X-ray crystallographic data were measured on a Stoe Stadivari diffractometer or Bruker APEX II Quazar diffractometer. The structures were solved and refined with SHELXT-2014[1] and refined against F_2 with a full-matrix least-squares algorithm using the SHELXL-2018/3[2] software. After full-matrix least-square refinement of the non-hydrogen atoms with anisotropic thermal parameters, the hydrogen atoms were placed in calculated positions using a riding model.

Theoretical calculations were performed using the Gaussian 16 software package.[3] The geometries of the molecules were optimized using the B3LYP[4] functional and 6-31G(d)[5] as the basis set. Nucleus independent chemical shifts (NICS)[6] values were calculated using the gauge-independent atomic orbital (GIAO)[7] method at the B3LYP/6-31G(d) level of theory. Highest occupied molecular orbitals (HOMOs) lowest unoccupied molecular orbitals (LUMOs) were visualized using the Avogadro[8] software package.

2 Synthetic Protocols

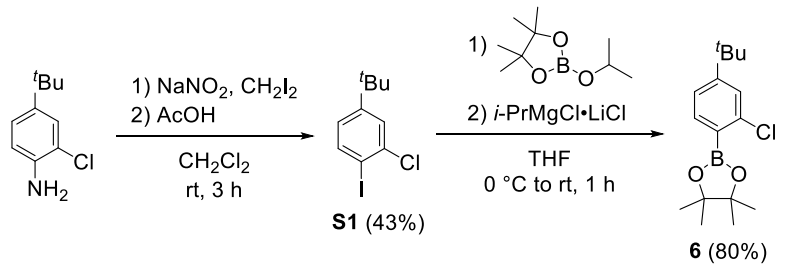

Scheme S1. Synthesis of boronic acid ester **6** from 4-(*tert*-butyl)-2-chloroaniline.

Compound **S1** was prepared according to a procedure described by *Stack* and coworkers for similar compounds.[9] The procedure for the synthesis of **6** was adapted from a general procedure for the synthesis of arylboronic esters disclosed by *Chavant* and coworkers.[10]

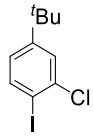

S1

4-*tert*-Butyl-2-chloro-1-iodobenzene (S1).
To a solution of 4-(*tert*-butyl)-2-chloroaniline (1.00 g, 5.44 mmol) in CH_2Cl_2 (90 mL) $NaNO_2$ (1.88 g, 27.2 mmol) and CH_2I_2 (0.88 mL, 2.92 g, 10.9 mmol) were added. After stirring for 20 min, acetic acid (6.54 g, 6.23 mL, 109 mmol) was added dropwise and the reaction mixture was stirred for 3 h at room temperature. The reaction mixture was treated with 10 wt.% aq. $Na_2S_2O_4$ (50 mL) and extracted with CH_2Cl_2 (100 mL). The combined organic layers were washed with saturated aq. NaCl (50 mL) and dried (Na_2SO_4). The solvent was removed under reduced pressure and the resulting red oil was purified by column chromatography (SiO_2, petroleum ether/EtOAc 50:1). Residual CH_2I_2 was removed under reduced pressure. Compound **S1** was obtained as a colorless oil (685 mg, 2.33 mmol, 43%).
R_f = 0.90 (SiO_2, petroleum ether/EtOAc 50:1).
^{1}H NMR (301 MHz, $CDCl_3$) δ 7.74 (d, J = 8.4, 1H), 7.46 (d, J = 2.3, 1H), 6.98 (dd, J = 8.4, 2.3, 1H), 1.29 (s, 9H) ppm.
^{13}C NMR (75 MHz, $CDCl_3$) δ 153.4, 139.6, 138.1, 126.7, 125.4, 93.9, 34.7, 30.9 ppm.

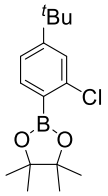

6

2-(4-*tert*-Butyl-2-chlorophenyl)-4,4,5,5-tetramethyl-1,3,2-dioxaborolane (6).

Under N_2 atmosphere **S1** (1.98 g, 6.71 mmol) and 2-isopropoxy-4,4,5,5-tetramethyl-1,3,2-dioxaborolane (1.75 g, 9.39 mmol) were dissolved in dry THF (20 mL). The reaction mixture was cooled to 0 °C and *i*-PrMgCl•LiCl (1.3M in THF, 6.19 mL, 1.17 g, 8.05 mmol) was added dropwise over the course of 5 min. The reaction mixture was stirred for 1 h at room temperature. Saturated aq. NH_4Cl was added to the reaction mixture, which was then extracted with EtOAc (3 × 25 mL). The combined organic layers were washed with saturated aq. NaCl (40 mL) and dried (Na_2SO_4). The solvent was removed under reduced pressure and the residue was purified by sublimation (5 × 10^{-2} mbar, 100 °C). Compound **6** (1.59 g, 5.40 mmol, 80%) was obtained as a colorless solid.

Mp 92–96 °C.

^{1}H NMR (400 MHz, $(CD_3)_2CO$) δ 7.64 (d, *J* = 7.8, 1H), 7.40 (d, *J* = 1.7, 1H), 7.36 (dd, *J* = 7.9, 1.8, 1H), 1.35 (s, 12H), 1.32 (s, 9H) ppm.

^{13}C NMR (101 MHz, $(CD_3)_2CO$) δ 156.8, 140.2, 137.5, 127.2, 124.0, 84.7, 35.5, 31.2, 25.1 ppm. (One signal coincident or not observed).

^{11}B NMR (128 MHz, $(CD_3)_2CO$) δ 30.60 ppm.

IR (ATR): $\tilde{\nu}$ 2964 (s), 2926 (m), 2867 (m), 1603 (s), 1535 (m), 1319 (s),1264 (m), 834 (m) cm^{-1}.

EI HRMS: calc. for $C_{16}H_{24}BClO_2$: 294.1552 [M^+], found 294.1563.

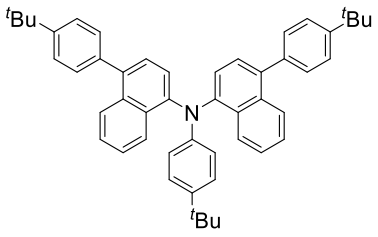

10

***N*,4-Bis(4-*tert*-butylphenyl)-*N*-[4-(4-*tert*-butylphenyl)naphthalen-1-yl]naphthalen-1-amine (10).**

In a microwave reaction vessel, a solution of compound **5** (50.0 mg, 89.4 μmol), [$Pd(PPh_3)_4$] (2.1 mg, 1.8 μmol), and 2-(4-*tert*-butylphenyl)-4,4,5,5-tetramethyl-1,3,2-dioxaborolane (69.8 mg, 268 μmol) in ethanol/toluene (1:2, vol./vol., 18 mL) was deoxygenated for 10 min under N_2 atmosphere. A deoxygenated solution of aq. K_2CO_3 (2 M, 1.12 mL, 309 mg, 2.23 mmol) was added, the reaction vessel was sealed and heated to 100 °C for 1 h. After the reaction mixture was allowed to cool to rt, H_2O (10 mL) was added. The orgainic phase was seperated and the aq. phase was extracted with CH_2Cl_2 (3 × 20 mL). The combined organic layers were washed with saturated aq. NaCl and dried (Na_2SO_4). The solvent was removed and the residue was purified by column chromatography (SiO_2, petroleum ether/CH_2Cl_2 5:1) followed by recrystallization from petroleum ether to obtain **10** (24.3 mg, 36.5 μmol, 41%) as a colorless solid.

R_f = 0.45 (SiO_2, petroleum ether/CH_2Cl_2 5:1).
Mp 200 °C.
^{1}H NMR (500 MHz, CD_2Cl_2) δ 8.26–8.23 (m, 2H), 8.02–7.97 (m, 2H), 7.56–7.51 (m, 4H), 7.47–7.44 (m, 4H), 7.42 (ddd, *J* = 8.4, 6.8, 1.4 Hz, 2H), 7.36 (ddd, *J* = 8.2, 6.8, 1.3 Hz, 2H), 7.32 (d, *J* = 7.6 Hz, 2H), 7.28 (d, *J* = 7.6 Hz, 2H), 7.22–7.17 (m, 2H), 6.79–6.74 (m, 2H), 1.42 (s, 18H), 1.29 (s, 9H) ppm.
^{13}C NMR (126 MHz, CD_2Cl_2) δ 150.6, 148.6, 145.0, 144.2, 138.0, 138.0, 133.7, 130.8, 130.2, 127.5, 127.2, 126.4, 126.3, 126.2, 125.6, 125.0, 124.7, 120.9, 34.9, 34.4, 31.6, 31.6 ppm.
IR (ATR): $\tilde{\nu}$ 3072 (w), 3033 (w), 2958 (m), 2866 (w), 1610 (w), 1577 (m), 1509 (s), 1426 (w), 1386 (s), 1262 (s), 826 (s), 763 (s) cm^{-1}.
UV/Vis (CH_2Cl_2, rt): λ_{max} in nm (ε in L mol^{-1} cm^{-1}) 274 (27200), 300 (16400), 361 (18200) nm.
MALDI HRMS (DCTB): calc. for $C_{50}H_{51}N$: *m/z* 665.4016 [M^+], found 665.4019.

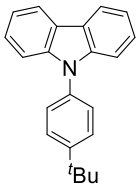

11

9-(4-*tert*-Butylphenyl)-9*H*-carbazole (11).[11]
In a sealed microwave reaction vessel, a mixture of 9*H*-carbazole (200 mg, 1.20 mmol), 1-*tert*-butyl-4-iodobenzene (600 µL, 882 mg, 3.39 mmol), activated copper (228 mg, 3.59 mmol), and K_2CO_3 (331 mg, 2.39 mmol) was heated to 200 °C for 20 h under nitrogen atmosphere. Afterwards, the reaction mixture was subjected to column chromatography (SiO_2, petroleum ether/CH_2Cl_2 10:1) to afford **11** (310 mg, 1.04 mmol, 87%) as a colorless solid.
R_f = 0.78 (SiO_2, petroleum ether/CH_2Cl_2 5:1).
Mp 191 °C (lit. 191–192 °C).[11a]
^{1}H NMR (301 MHz, $CDCl_3$) δ 8.16 (dt, *J* = 7.7, 1.1 Hz, 2H), 7.64–7.59 (m, 2H), 7.52–7.47 (m, 2H), 7.47–7.37 (m, 4H), 7.32–7.26 (m, 2H), 1.44 (s, 9H) ppm.
^{13}C NMR (101 MHz, $CDCl_3$) δ 150.6, 141.2, 135.1, 126.9, 126.8, 126.0, 123.4, 120.4, 119.9, 110.0, 34.9, 31.6 ppm.
IR (ATR): $\tilde{\nu}$ 3045 (w), 2960 (m), 1626 (w), 1592 (m), 1519 (s), 1451 (s), 1232 (s), 830 (m), 748 (s), 723 (s) cm^{-1}.
UV/Vis (CH_2Cl_2, rt): λ_{max} in nm (ε in L mol^{-1} cm^{-1}) 242 (48200), 263 (21000), 286 (16900), 294 (19200), 318 (2990), 329 (4310), 342 (4680) nm.
EI HRMS: calc. for $C_{22}H_{21}N$: 299.1669 [M^+], found 299.1685.
Spectral data consistent with those reported in literature.[11b]

3 Nuclear Magnetic Resonance Spectra

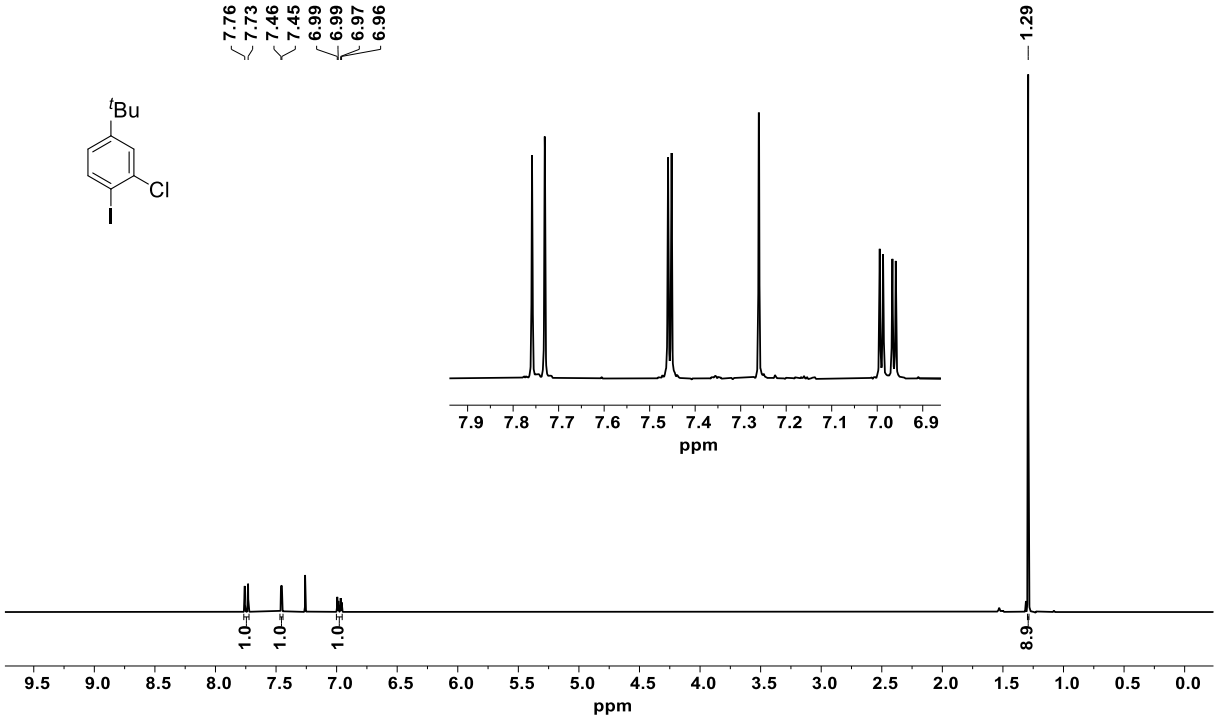

Figure S1 ^{1}H NMR spectrum of **S1** (301 MHz, $CDCl_3$, rt).

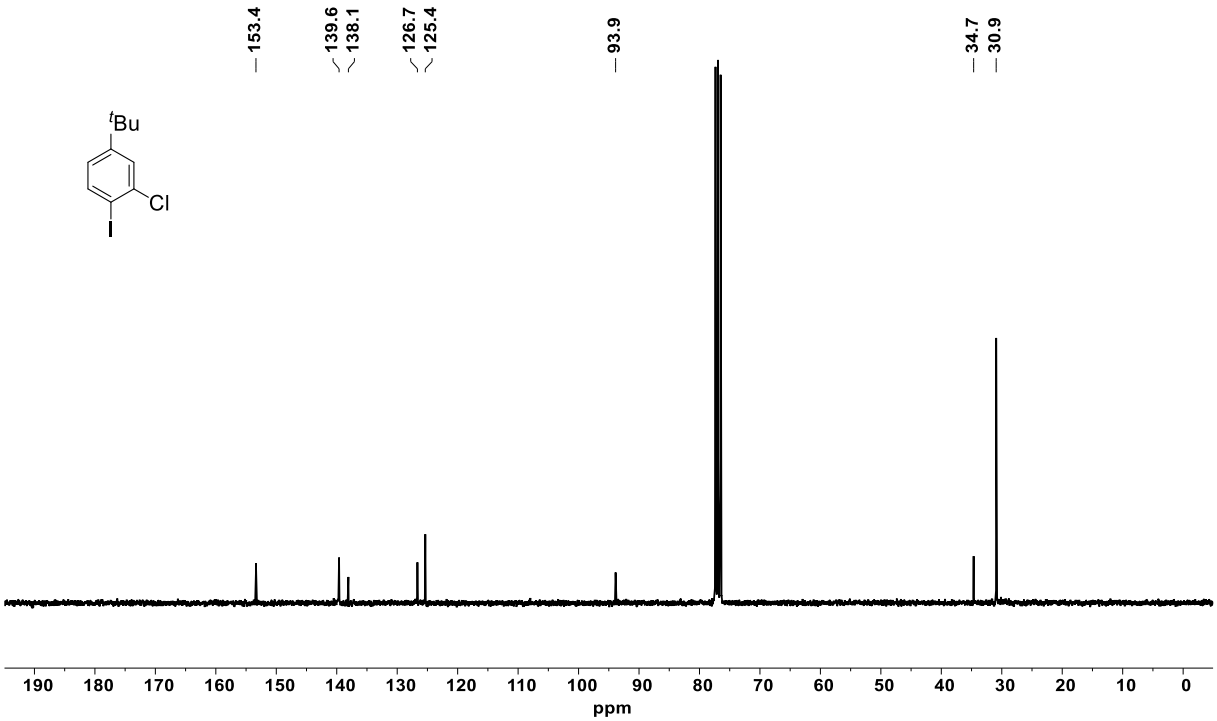

Figure S2. ^{13}C NMR spectrum of **S1** (75 MHz, $CDCl_3$, rt).

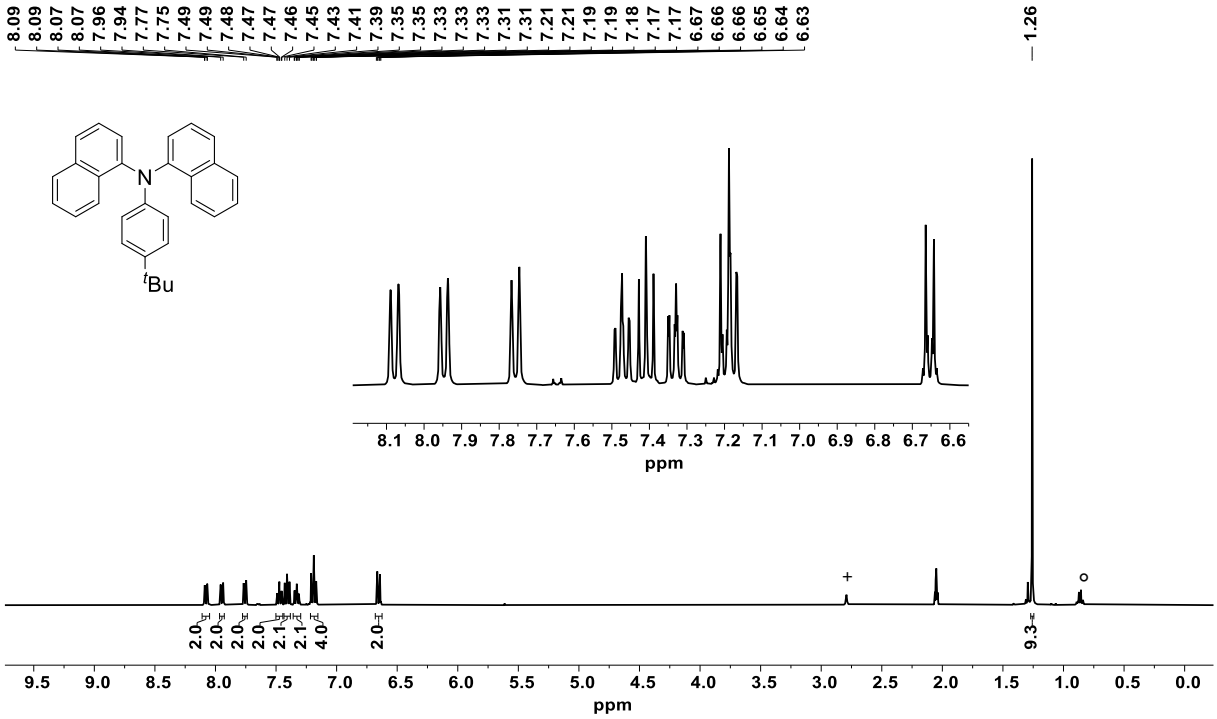

Figure S3 ^{1}H NMR spectrum of **4** (400 MHz, $(CD_3)_2CO$, rt); ° petroleum ether, ⁺ water.

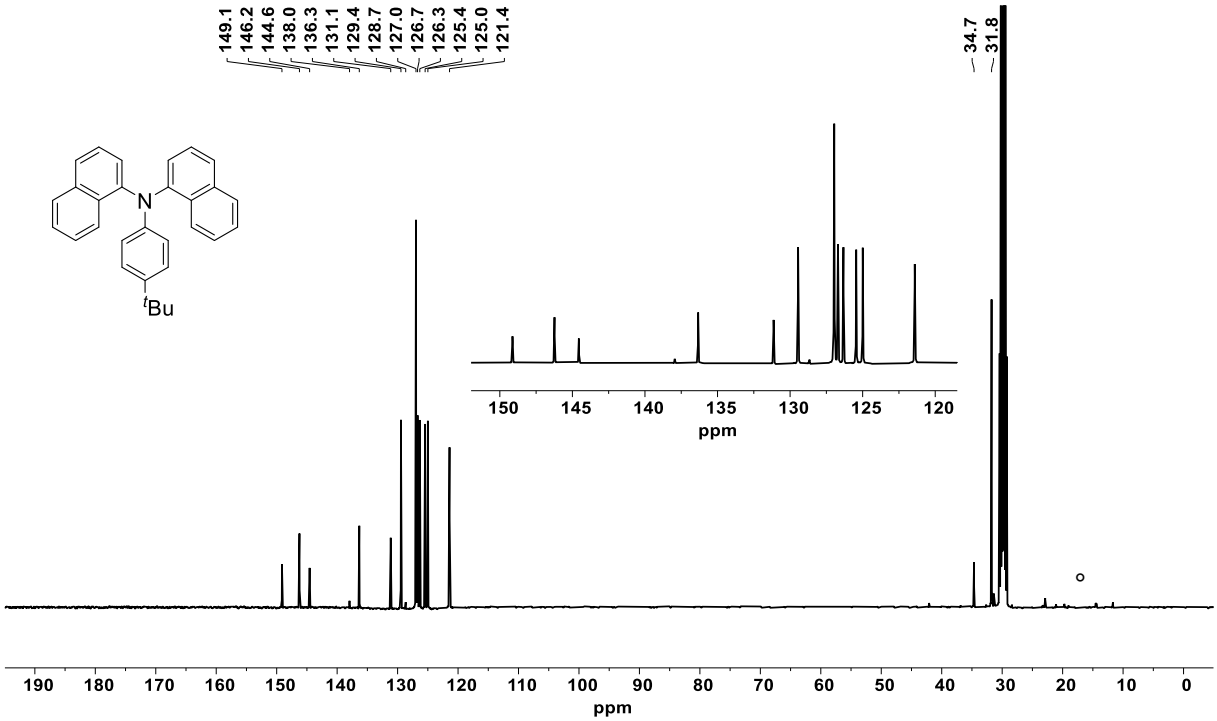

Figure S4 ^{13}C NMR spectrum of **4** (101 MHz, $(CD_3)_2CO$, rt); ° petroleum ether.

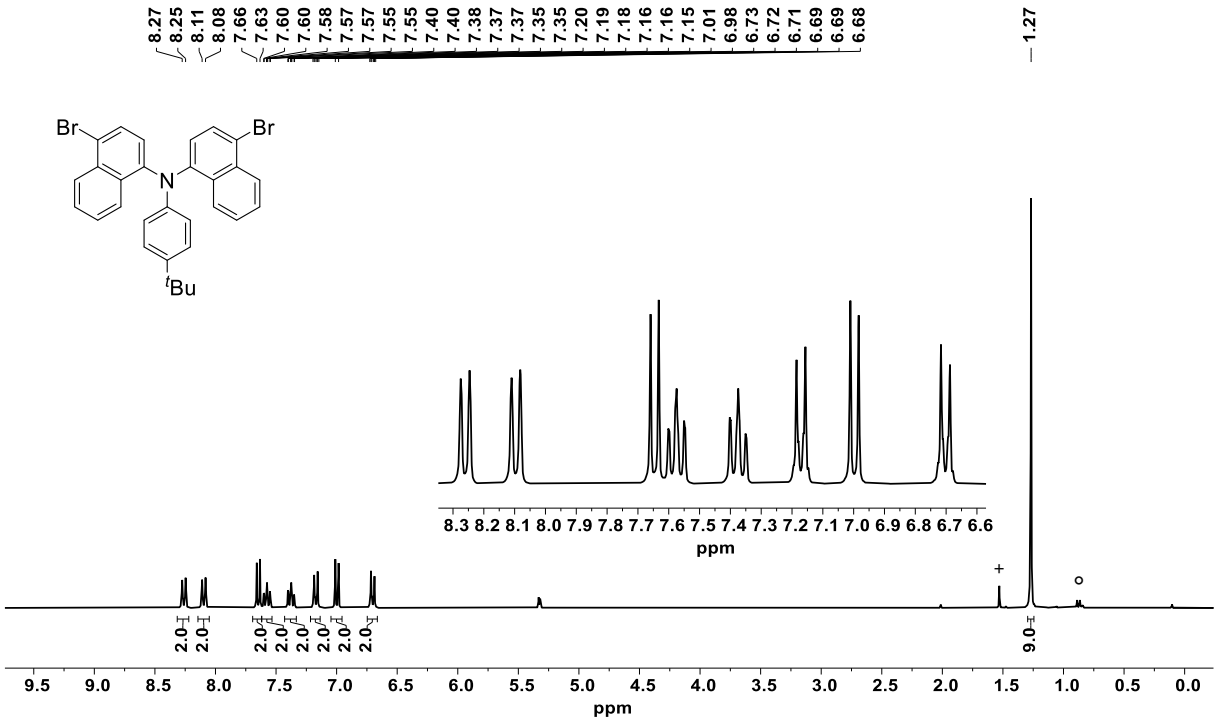

Figure S5 ^{1}H NMR spectrum of **5** (300 MHz, CD_2Cl_2, rt); ° petroleum ether, $^{+}$ H_2O.

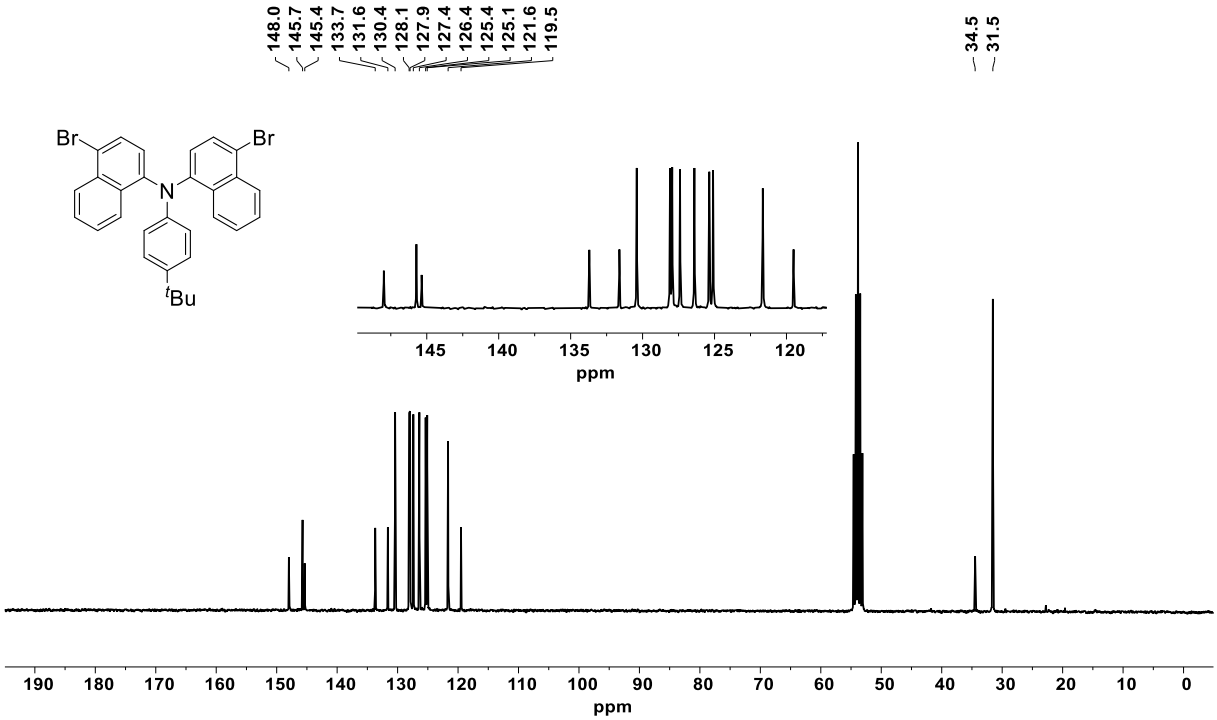

Figure S6 ^{13}C NMR spectrum of **5** (75 MHz, CD_2Cl_2, rt).

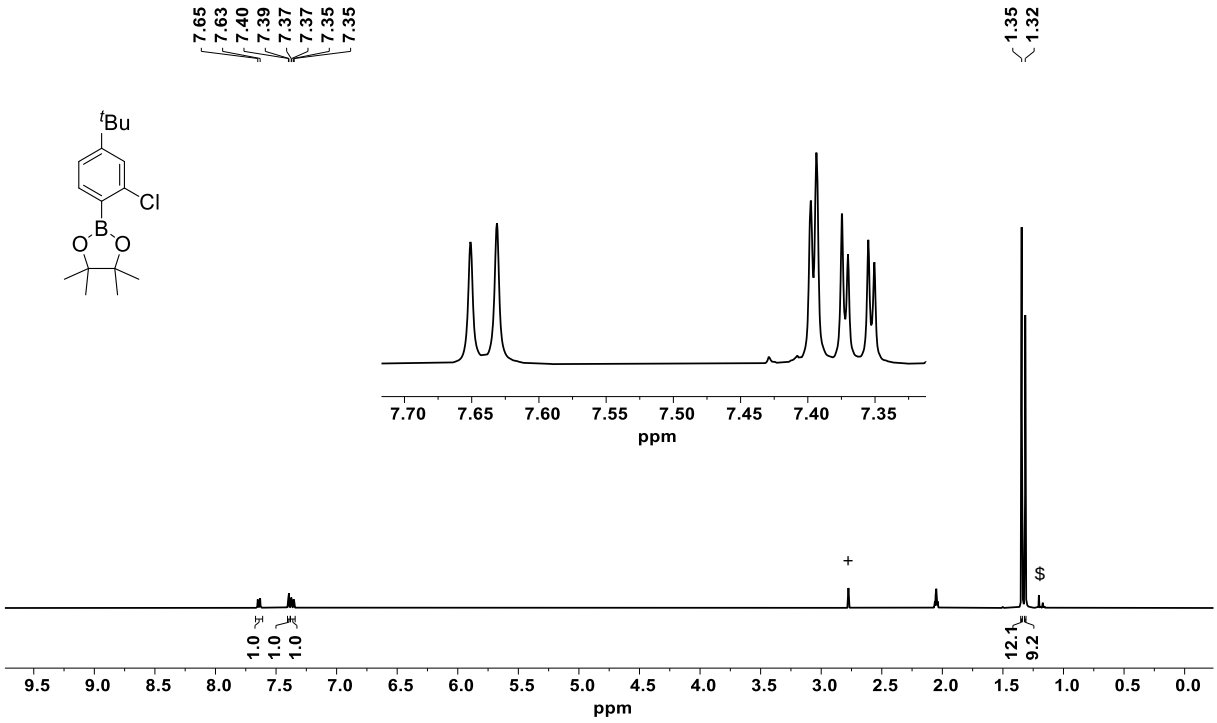

Figure S7 ^{1}H NMR spectrum of **6** (400 MHz, $(CD_3)_2CO$, rt); $^{\$}$ unknown impurity, $^{+}$ H_2O.

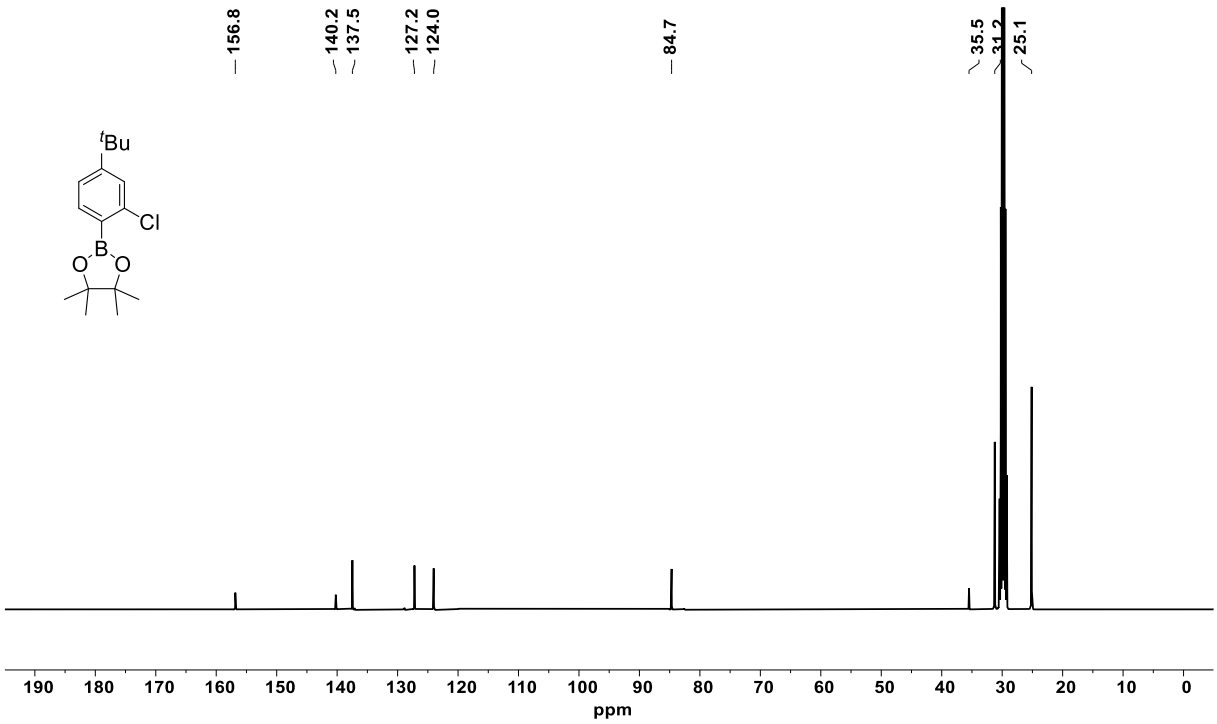

Figure S8 ^{13}C NMR spectrum of **6** (101 MHz, $(CD_3)_2CO$, rt).

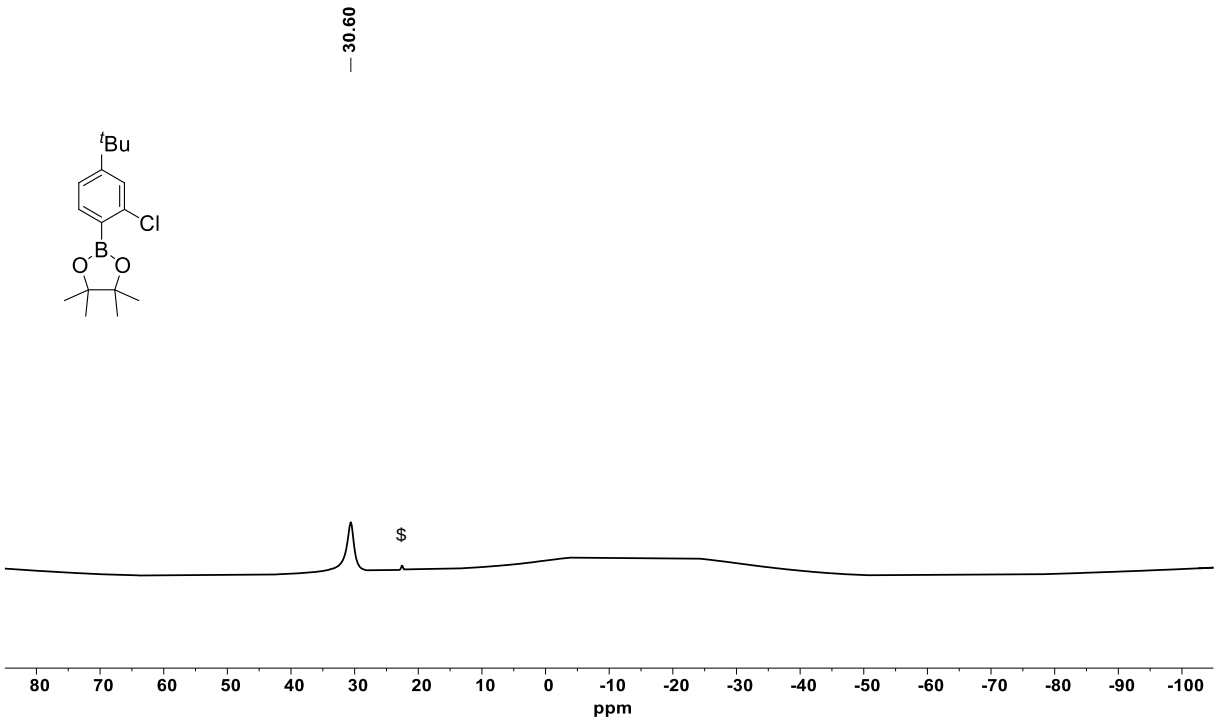

Figure S9 ^{11}B NMR spectrum of **6** (128 MHz, $(CD_3)_2CO$, rt); $ unknown impurity.

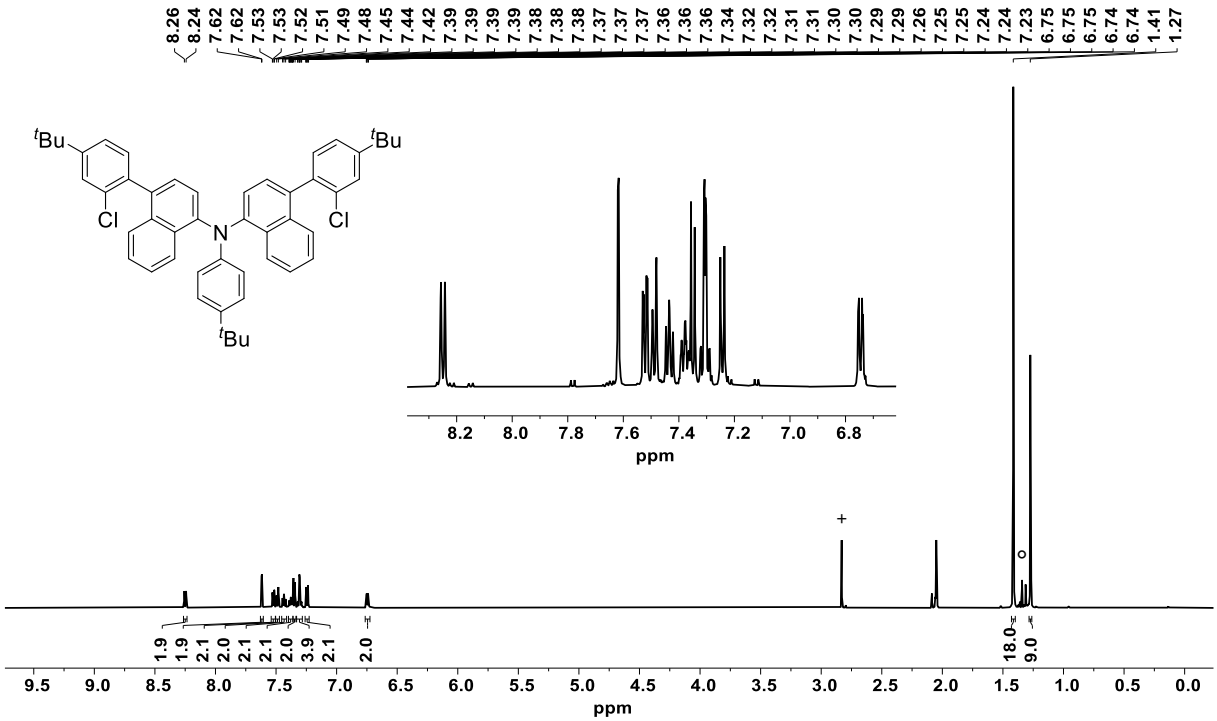

Figure S10 ^{1}H NMR spectrum of **7** (600 MHz, $(CD_3)_2CO$, rt); ° petroleum ether, $^{+}$ water.

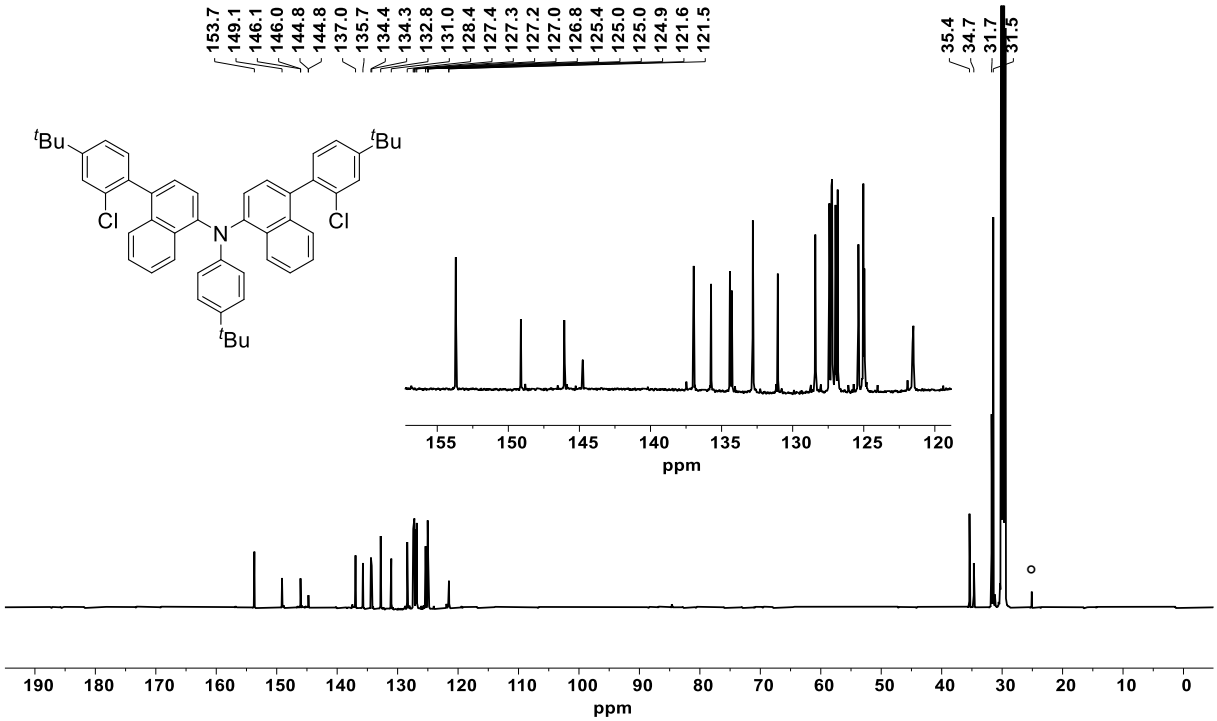

Figure S11 ^{13}C NMR spectrum of **7** (151 MHz, $(CD_3)_2CO$, rt); ° petroleum ether.

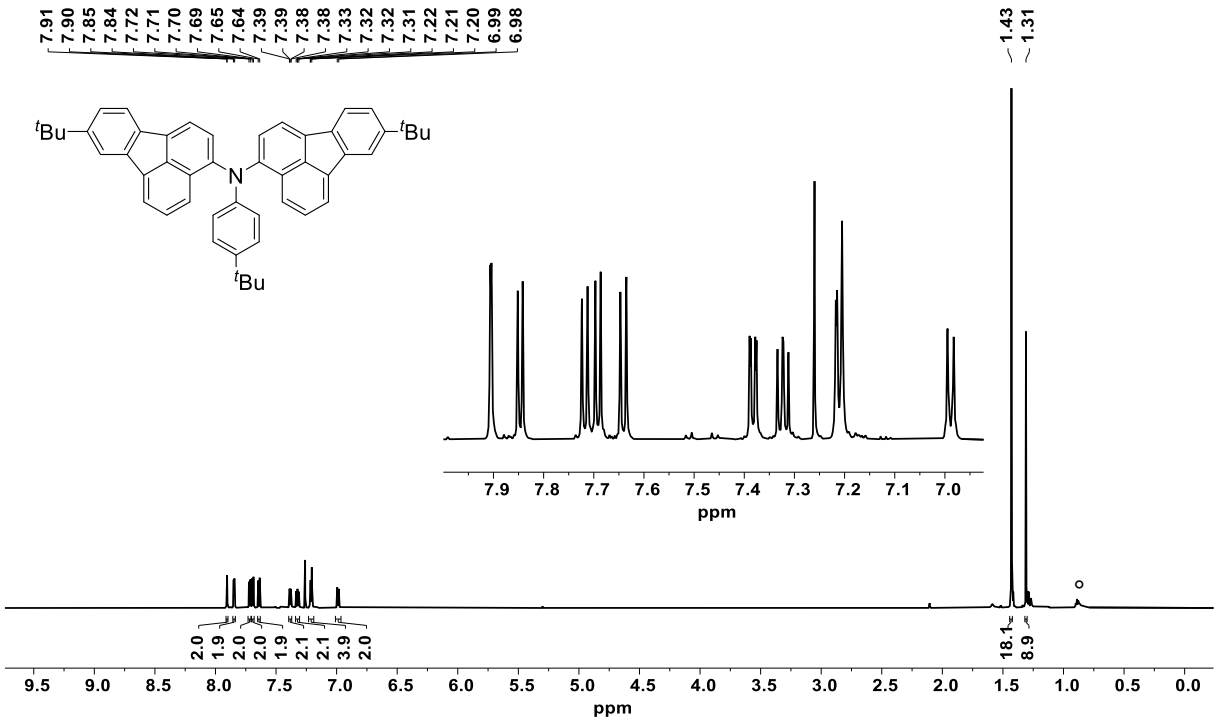

Figure S12 ^{1}H NMR spectrum of **8** (700 MHz, $CDCl_3$, rt); ° petroleum ether.

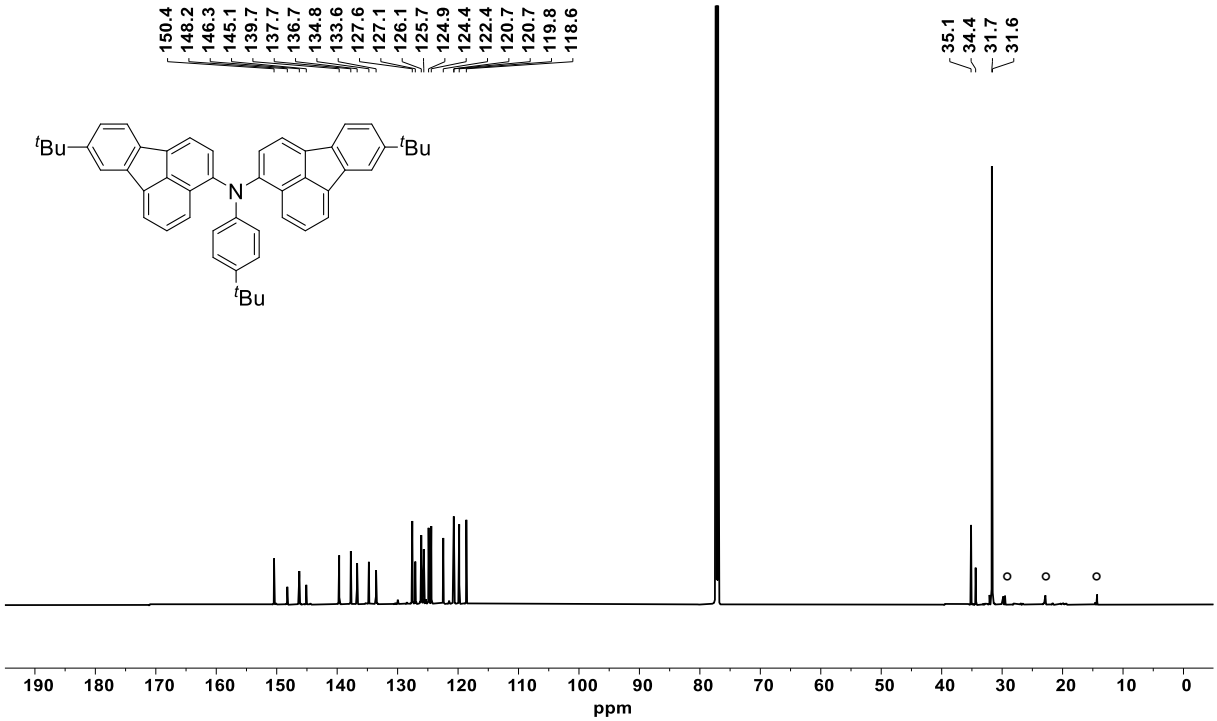

Figure S13 ^{13}C NMR spectrum of **8** (176 MHz, $CDCl_3$, rt); ° petroleum ether.

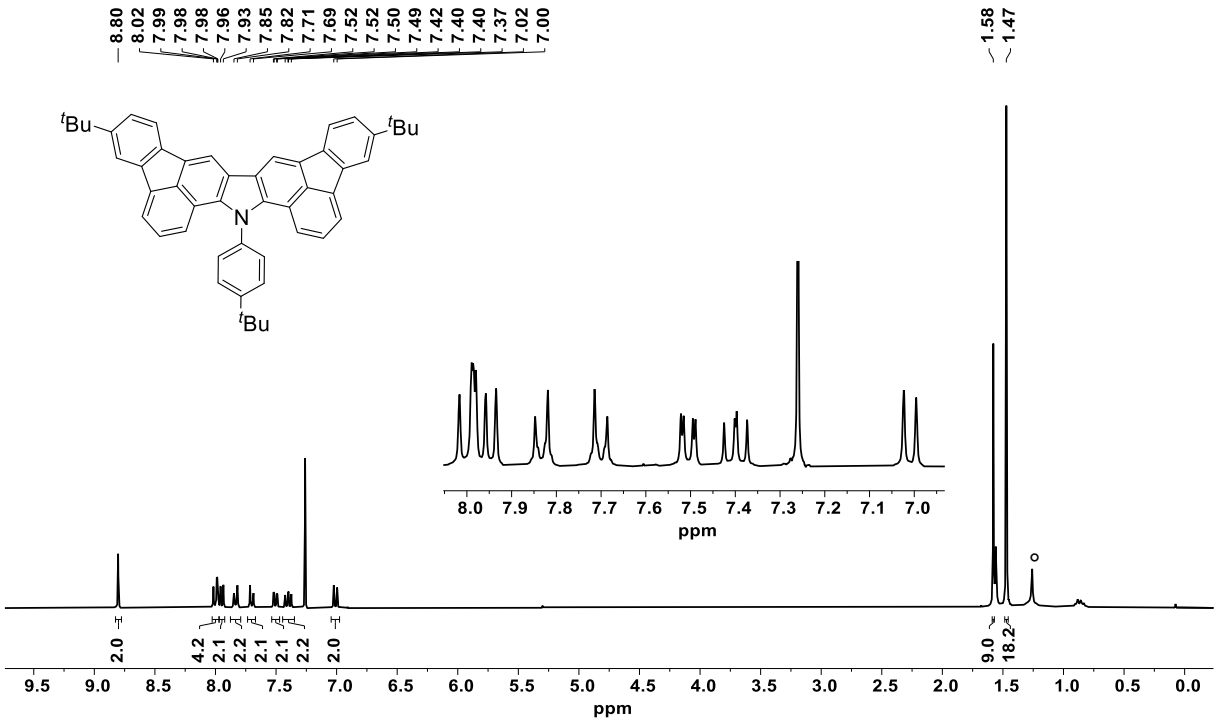

Figure S14 ^{1}H NMR spectrum of **9** (301 MHz, $CDCl_3$, rt); ° petroleum ether.

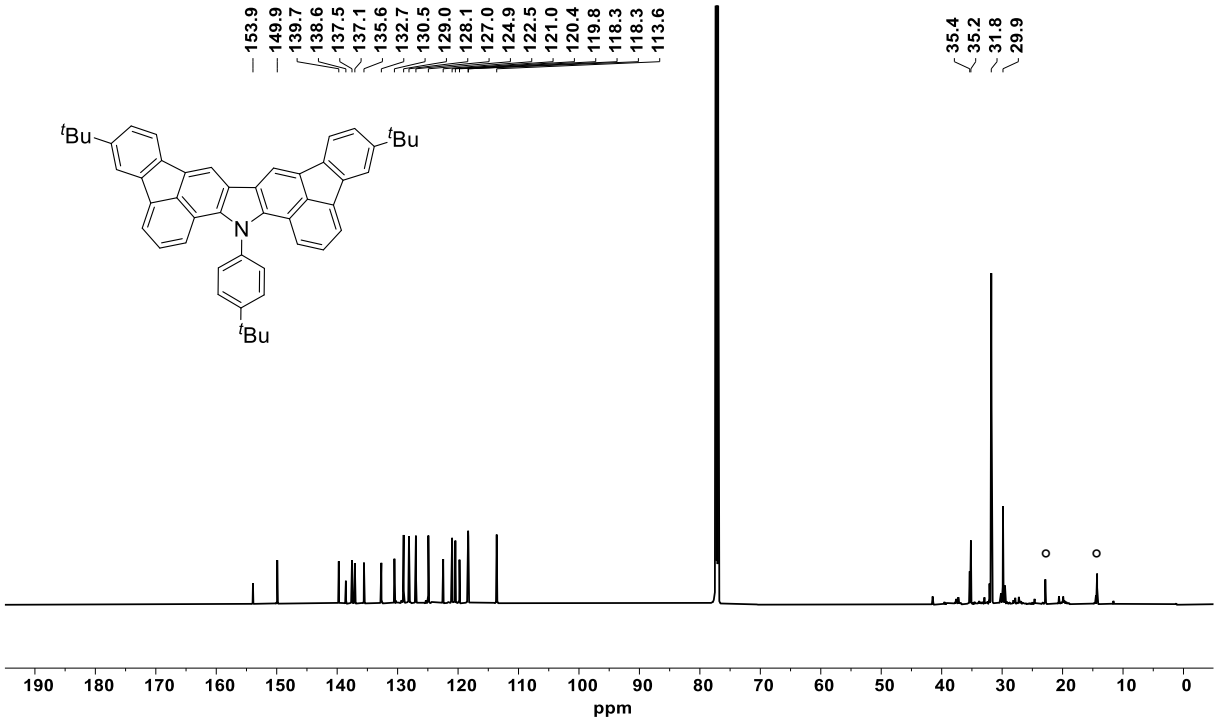

Figure S15 ^{13}C NMR spectrum of **9** (176 MHz, $CDCl_3$, rt), ° petroleum ether.

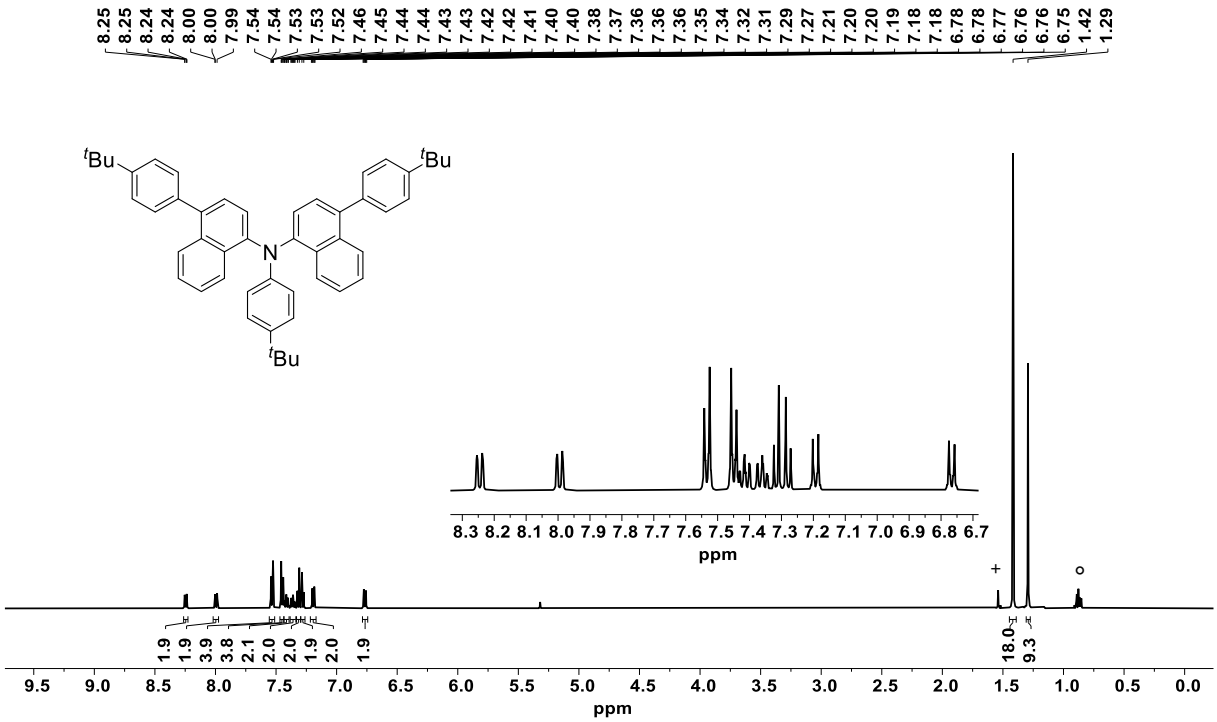

Figure S16 ^{1}H NMR spectrum of **10** (500 MHz, CD_2Cl_2, rt); ° petroleum ether, $^{+}$ water.

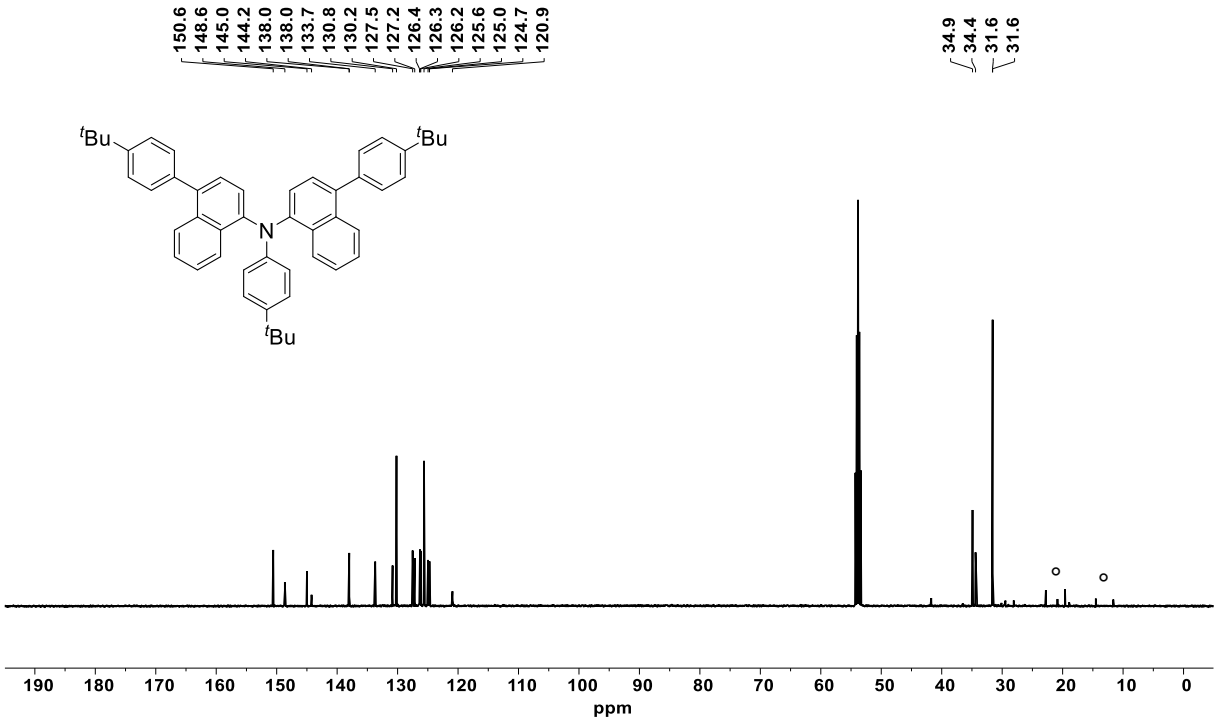

Figure S17 ^{13}C NMR spectrum of **10** (126 MHz, CD_2Cl_2, rt); ° petroleum ether.

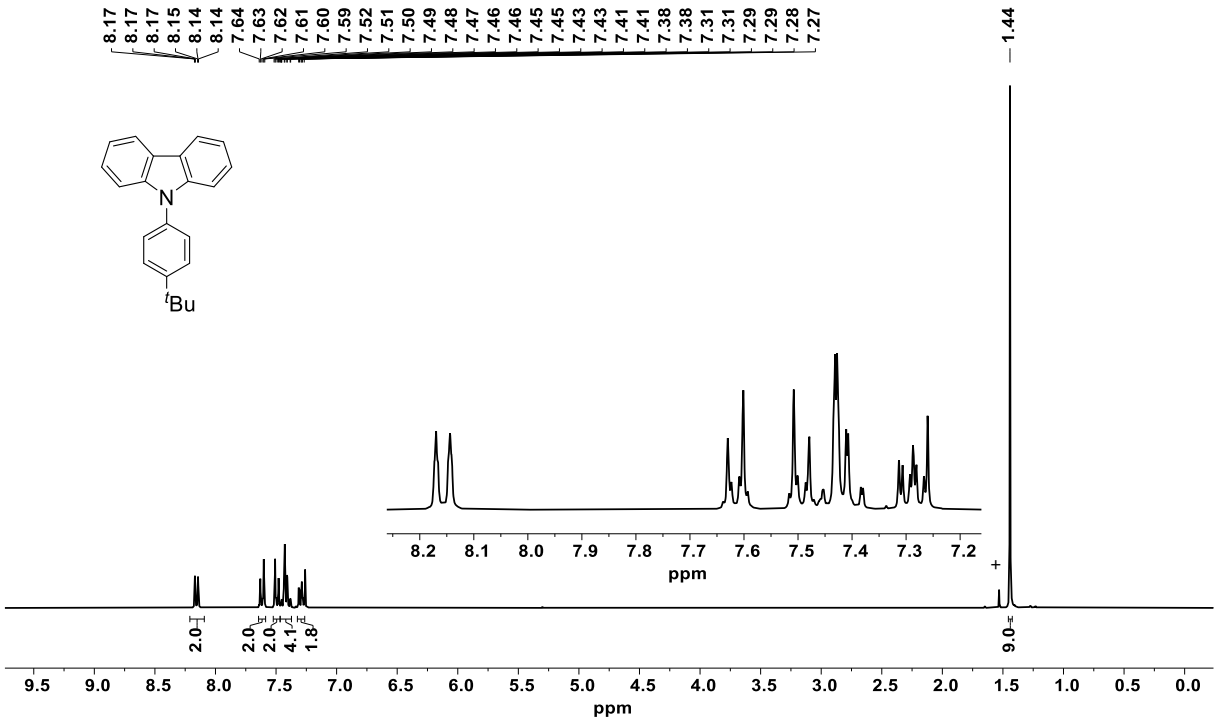

Figure S18 ^{1}H NMR spectrum of **11** (301 MHz, $CDCl_3$, rt); $^{+}$ water.

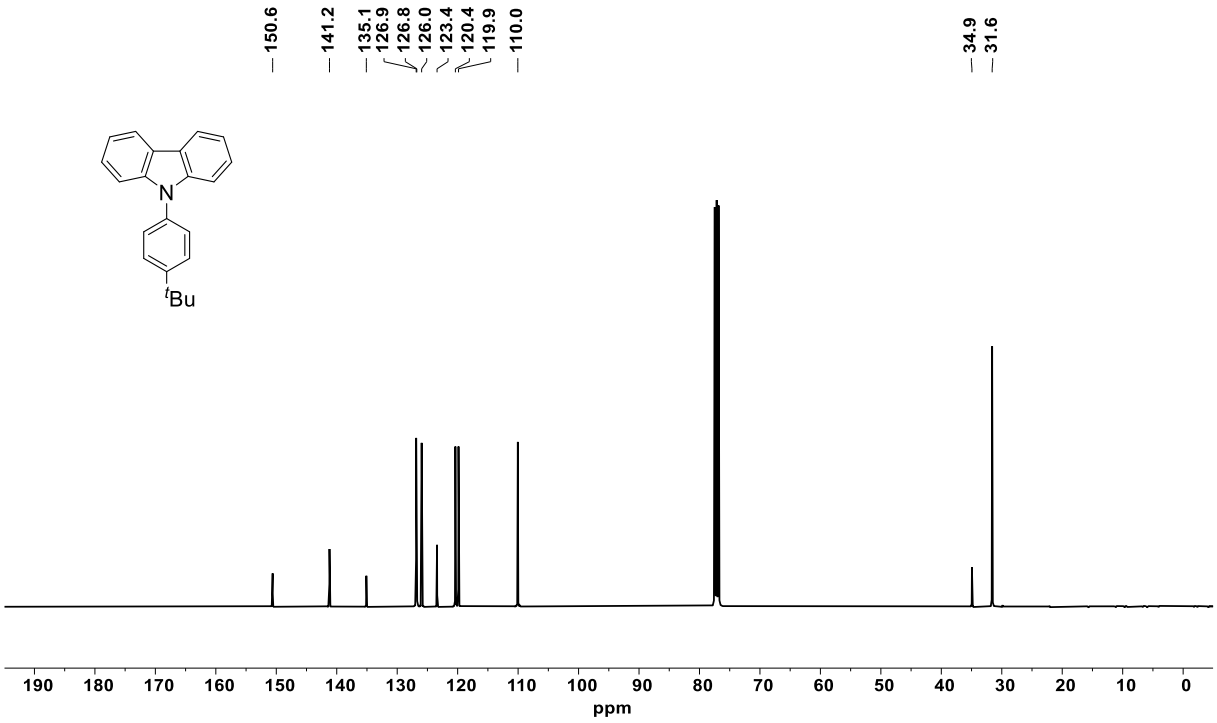

Figure S19 ^{13}C NMR spectrum of **11** (101 MHz, $CDCl_3$, rt).

4 Crystallographic Data Collection and Structure Determination

Crystal data for compound 5

Single crystals of compound **5** were obtained at rt from CH_2Cl_2/MeOH by slow evaporation. CCDC 2170907 contains the supplementary crystallographic data for this paper. The data can be obtained free of charge from The Cambridge Crystallographic Data Centre via www.ccdc.cam.ac.uk/structures.

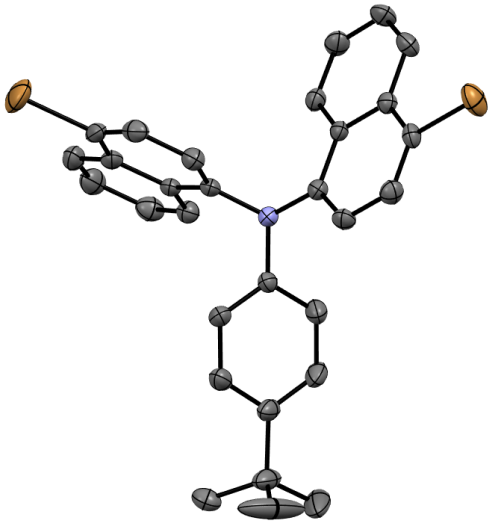

Figure S20 X-ray crystal structure of compound **5** (50% probability level, H-atoms omitted).

Table S1 Crystallographic data of **5**.

Empirical formula	$C_{30}H_{25}Br_2N$	
Formula weight	559.33	
Temperature	200(2) K	
Wavelength	0.71073 Å	
Crystal system	monoclinic	
Space group	$P2_1/n$	
Z	4	
Unit cell dimensions	a = 9.9459(5) Å	α = 90 deg.
	b = 21.7625(10) Å	β = 107.8511(10) deg.
	c = 12.1602(6) Å	γ = 90 deg.
Volume	2505.3(2) Å^3	
Density (calculated)	1.48 g/cm^3	
Absorption coefficient	3.25 mm^{-1}	
Crystal shape	column	
Crystal size	0.354 x 0.103 x 0.098 mm^3	
Crystal color	yellow	
Theta range for data collection	1.9 to 29.2 deg.	
Index ranges	-12≤h≤13, -29≤k≤29, -16≤l≤16	
Reflections collected	28853	

Independent reflections	6308 (R(int) = 0.0541)
Observed reflections	4140 ($I > 2\sigma(I)$)
Absorption correction	semi-empirical from equivalents
Max. and min. transmission	0.77 and 0.58
Refinement method	full-matrix least-squares on F^2
Data/restraints/parameters	6308 / 0 / 301
Goodness-of-fit on F^2	1.02
Final R indices (I>2sigma(I))	R1 = 0.043, wR2 = 0.076
Largest diff. peak and hole	0.55 and -0.65 $eÅ^{-3}$

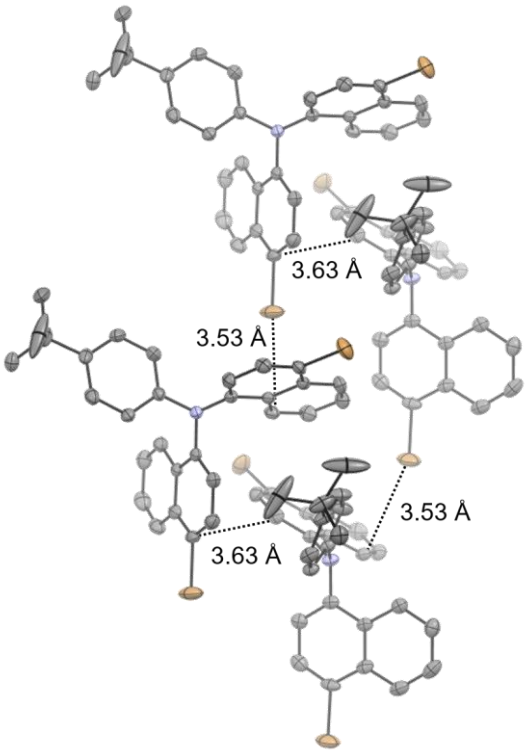

Figure S21 Solid state packing of compound **5** (50% probability level, H-atoms omitted).

Crystal data for compound 9

Single crystals of compound **9** were obtained at rt from CH_2Cl_2/MeOH by slow evaporation. CCDC 2170908 contains the supplementary crystallographic data for this paper. The data can be obtained free of charge from The Cambridge Crystallographic Data Centre via www.ccdc.cam.ac.uk/structures.

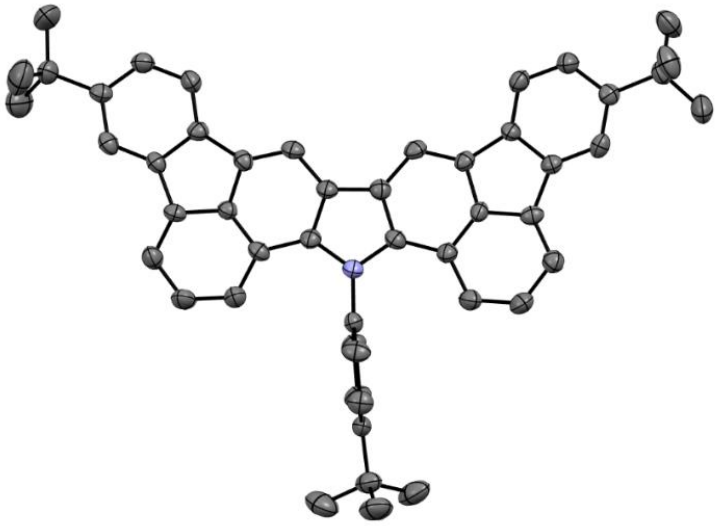

Figure S22 X-ray crystal structure of compound **9** (50% probability level, H-atoms omitted).

Table S2 Crystallographic data of **9**.

Empirical formula	$C_{50}H_{45}N$	
Formula weight	659.87	
Temperature	200(2) K	
Wavelength	0.71073 Å	
Crystal system	triclinic	
Space group	$P\bar{1}$	
Z	2	
Unit cell dimensions	a = 10.6513(9) Å	α = 78.689(2) deg.
	b = 10.9541(9) Å	β = 79.654(2) deg.
	c = 16.8546(14) Å	γ = 77.539(2) deg.
Volume	1863.4(3) $Å^3$	
Density (calculated)	1.18 g/cm^3	
Absorption coefficient	0.07 mm^{-1}	
Crystal shape	plate	
Crystal size	0.225 x 0.120 x 0.050 mm^3	
Crystal color	yellow	
Theta range for data collection	1.9 to 19.2 deg.	
Index ranges	-9≤h≤9, -10≤k≤10, -15≤l≤15	
Reflections collected	13335	
Independent reflections	3070 (R(int) = 0.0447)	
Observed reflections	2320 (I > 2\s(I))	
Absorption correction	semi-empirical from equivalents	
Max. and min. transmission	0.74 and 0.68	
Refinement method	full-matrix least-squares on F^2	
Data/restraints/parameters	3070 / 0 / 469	

Goodness-of-fit on F^2	1.02
Final R indices ($I>2\sigma(I)$)	R1 = 0.047, wR2 = 0.112
Largest diff. peak and hole	0.33 and -0.21 eÅ^{-3}

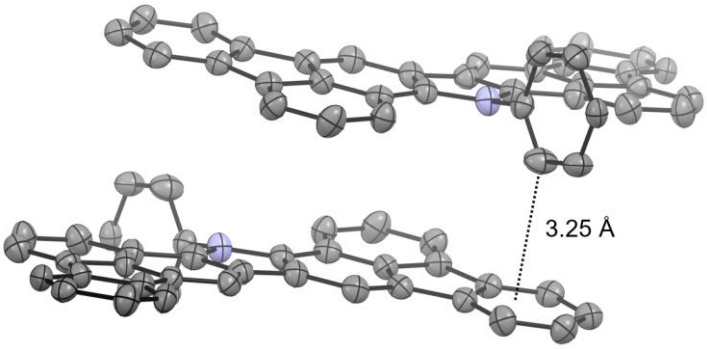

Figure S23 Edge to face C(sp^2)–H···π-interactions in the crystal packing of molecule **9** (50% probability level, H-atoms omitted).

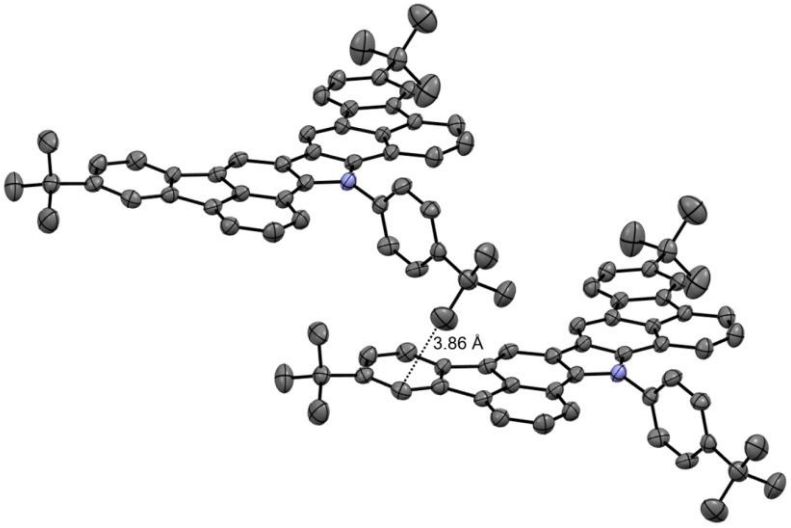

Figure S24 C(sp^3)–H···π-interactions in the crystal packing of molecule **9** (50% probability level, H-atoms omitted).

5 UV/Vis Spectroscopy

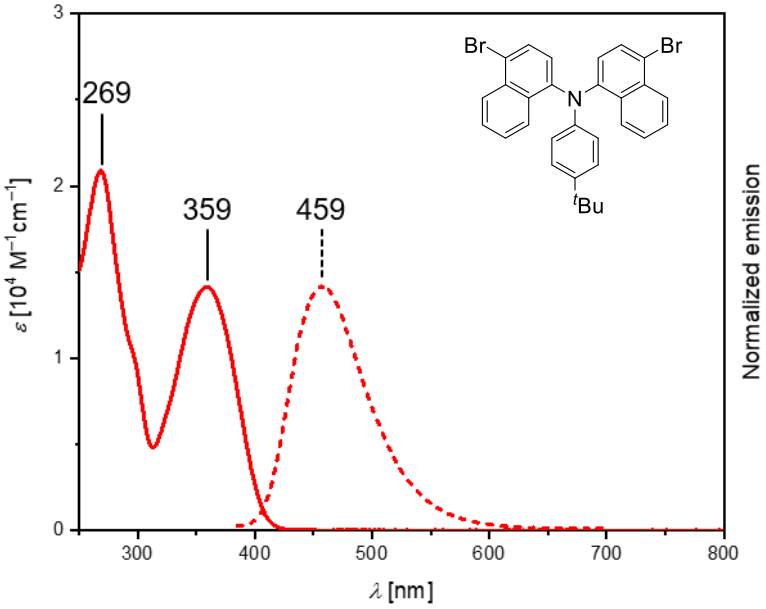

Figure S25 UV/Vis absorption (solid line) and emission (dashed line) spectrum of **5** recorded in CH_2Cl_2 at room temperature.

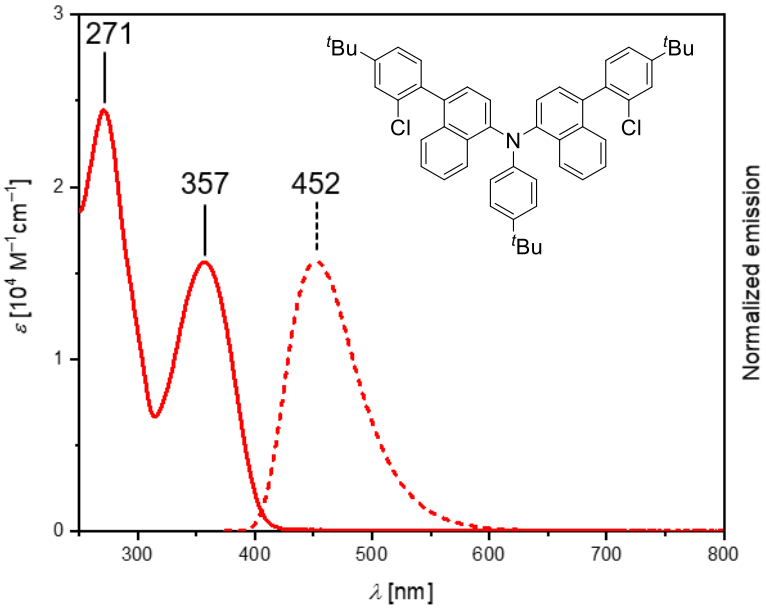

Figure S26 UV/Vis absorption (solid line) and emission (dashed line) spectrum of **7** recorded in CH_2Cl_2 at room temperature.

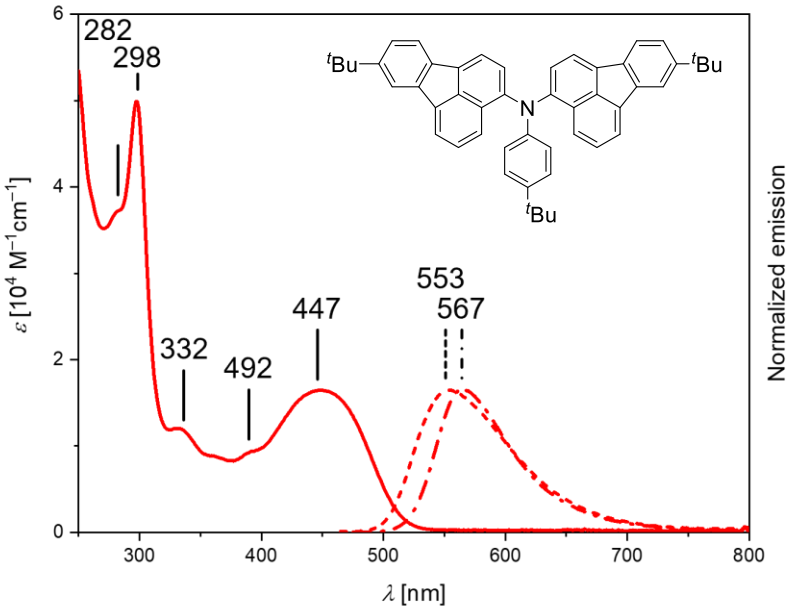

Figure S27 UV/Vis absorption (solid line) and emission (dashed line) spectrum of **8** recorded in CH_2Cl_2 at room temperature. UV/Vis solid state emission of **8** (dashed and dotted line) recorded at room temperature.

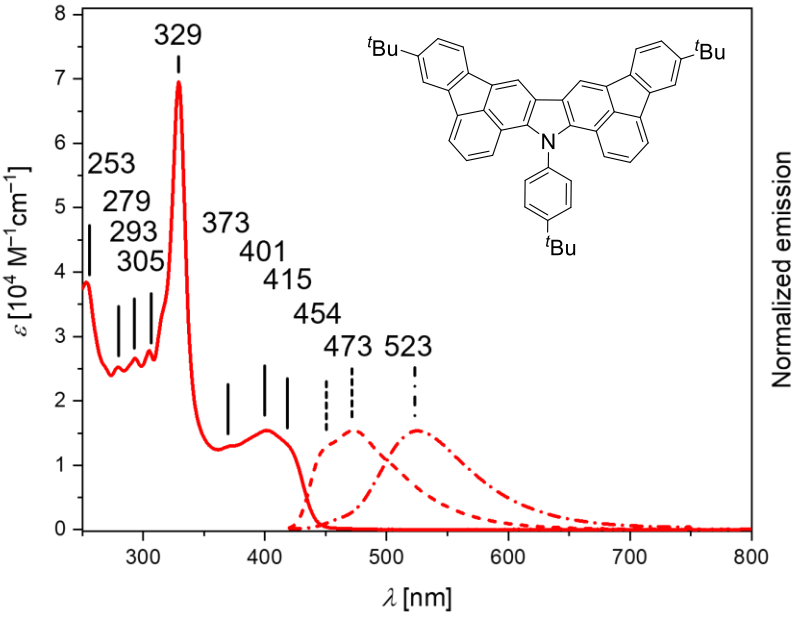

Figure S28 UV/Vis absorption (solid line) and emission (dashed line) spectrum of **9** recorded in CH_2Cl_2 at room temperature. UV/Vis solid state emission of **9** (dashed and dotted line) recorded at room temperature.

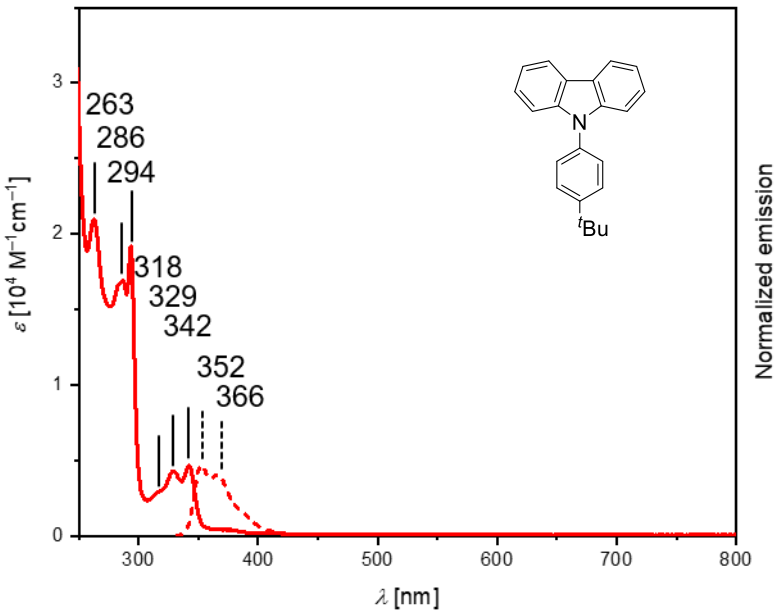

Figure S29 UV/Vis absorption (solid line) and emission (dashed line) spectrum of **11** recorded in CH_2Cl_2 at room temperature.

6 Cyclic Voltammetry

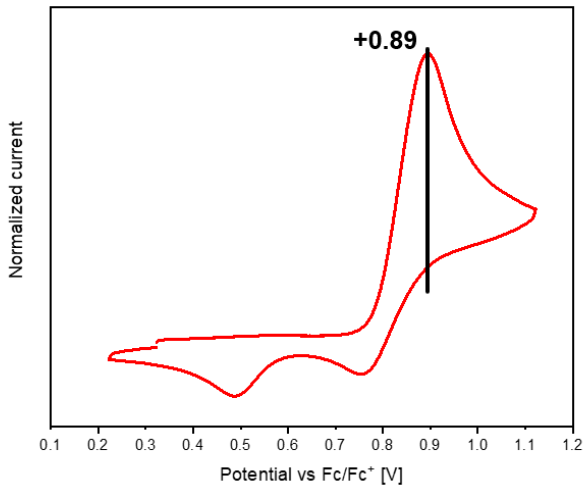

Figure S30 Cyclic voltammetry of compound **11** measured in CH_2Cl_2 at room temperature with *n*-Bu_4NPF_6 as the supporting electrolyte. The scan rate (ν) was set to 100 mVs^{-1} and the potentials are referenced against Fc/Fc^+.

7 Theoretical Calculations

Table S3 NICS(0), NICS(+1), and NICS(–1) values of rings A–F in compounds **8**, **9**, and **11**. NICS(+1) values visualized as red dots inside the rings of **8**, **9**, and **11**. The size of the dots represents the relative aromaticity of the rings. Top left: Assignment of the rings A–F.

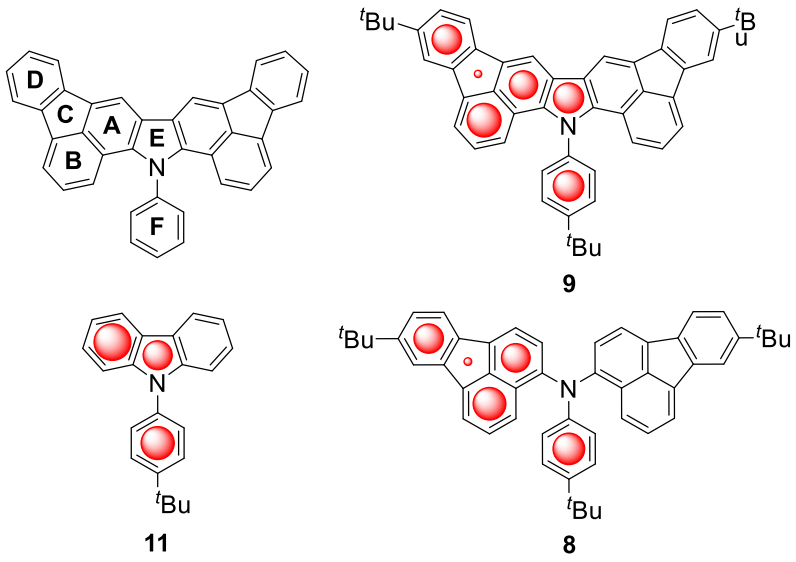

Ring	Compound **8**			Compound **9**			Compound **11**		
	NICS(0)	NICS(+1)	NICS(-1)	NICS(0)	NICS(+1)	NICS(-1)	NICS(0)	NICS(+1)	NICS(-1)
A	–7.1	–8.1	–8.5	–7.3	–8.4	–8.4	–10.8	–11.3	–11.6
B	–8.5	–10.2	–10.0	–9.2	–10.6	–10.6			
C	+4.0	–0.4	–0.6	+3.8	–0.5	–0.5			
D	–7.0	–8.9	–8.9	–7.0	–8.9	–8.9			
E				–10.4	–9.1	–9.1	–9.5	–8.7	–8.7
F	–8.6	–9.7	–9.7	–8.5	–9.2	–9.2	–9.0	–10.3	–10.3

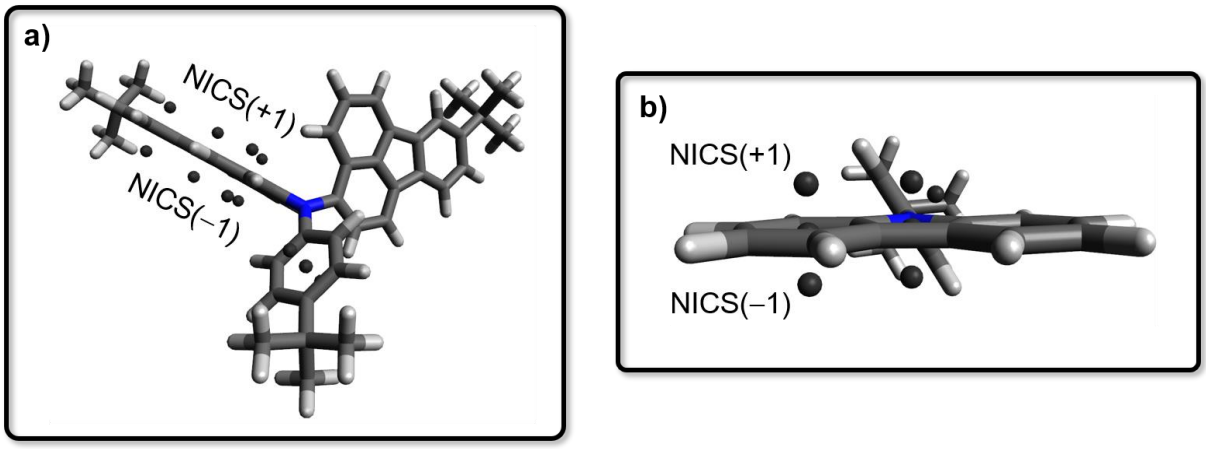

Figure S31 Placement of dummy atoms for the calculation of NICS(+1) and NICS(–1) values. a) Compound **8**. b) Compound **11**.

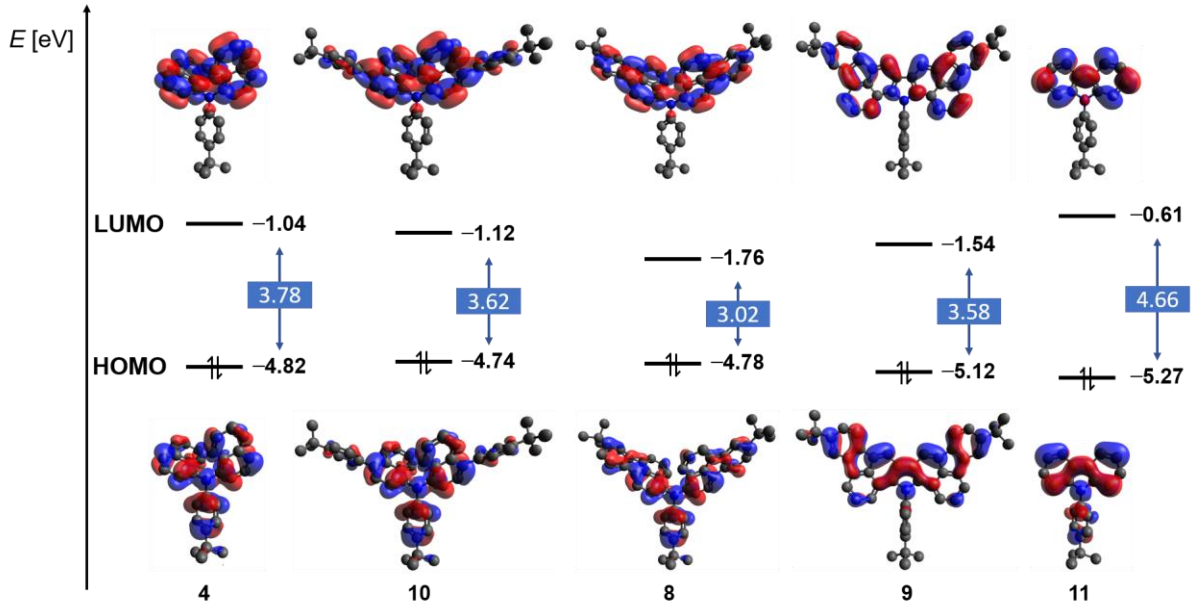

Figure S32 Frontier molecular orbitals of compounds **4** and **8**–**11**.

8 References

[1] G. M. Sheldrick, *Acta Cryst A* **2015**, *71*, 3–8.

[2] G. M. Sheldrick, *Acta Cryst C* **2015**, *71*, 3–8.

[3] M. J. Frisch, G. W. Trucks, H. B. Schlegel, G. E. Scuseria, M. A. Robb, J. R. Cheeseman, G. Scalmani, V. Barone, G. A. Petersson, H. Nakatsuji, X. Li, M. Caricato, A. V. Marenich, J. Bloino, B. G. Janesko, R. Gomperts, B. Mennucci, H. P. Hratchian, J. V. Ortiz, A. F. Izmaylov, J. L. Sonnenberg, D. Williams-Young, F. Ding, F. Lipparini, F. Egidi, J. Goings, B. Peng, A. Petrone, T. Henderson, D. Ranasinghe, V. G. Zakrzewski, J. Gao, N. Rega, G. Zheng, W. Liang, M. Hada, M. Ehara, K. Toyota, R. Fukuda, J. Hasegawa, M. Ishida, T. Nakajima, Y. Honda, O. Kitao, H. Nakai, T. Vreven, K. Throssell, J. A. Montgomery, Jr, J. E. Peralta, F. Ogliaro, M. J. Bearpark, J. J. Heyd, E. N. Brothers, K. N. Kudin, V. N. Staroverov, T. A. Keith, R. Kobayashi, J. Normand, K. Raghavachari, A. P. Rendell, J. C. Burant, S. S. Iyengar, J. Tomasi, M. Cossi, J. M. Millam, M. Klene, C. Adamo, R. Cammi, J. W. Ochterski, R. L. Martin, K. Morokuma, O. Farkas, J. B. Foresman, D. J. Fox, *Gaussian 16;* Gaussian, Inc, Wallingford CT, **2016**.

[4] a) A. D. Becke, *Phys. Rev. A* **1988**, *38*, 3098–3100; b) C. Lee, W. Yang, R. G. Parr, *Phys. Rev. B Condens. Matter* **1988**, *37*, 785–789; c) A. D. Becke, *Appl. Phys. Lett.* **1993**, *98*, 5648–5652.

[5] a) W. J. Hehre, R. Ditchfield, J. A. Pople, *Appl. Phys. Lett.* **1972**, *56*, 2257–2261; b) P. C. Hariharan, J. A. Pople, *Theoret. Chim. Acta* **1973**, *28*, 213–222.

[6] a) P. v. R. Schleyer, C. Maerker, A. Dransfeld, H. Jiao, N. J. R. van Eikema Hommes, *J. Am. Chem. Soc.* **1996**, *118*, 6317–6318; b) P. v. R. Schleyer, H. Jiao, N. J. R. E. van Hommes, V. G. Malkin, O. L. Malkina, *J. Am. Chem. Soc.* **1997**, *119*, 12669–12670; c) Z. Chen, C. S. Wannere, C. Corminboeuf, R. Puchta, P. v. R. Schleyer, *Chem. Rev.* **2005**, *105*, 3842–3888.

[7] a) F. London, *J. Phys. Radium* **1937**, *8*, 397–409; b) R. McWeeny, *Phys. Rev.* **1962**, *126*, 1028–1034; c) R. Ditchfield, *Mol. Phys* **1974**, *27*, 789–807; d) K. Wolinski, J. F. Hinton, P. Pulay, *J. Am. Chem. Soc.* **1990**, *112*, 8251–8260; e) J. R. Cheeseman, G. W. Trucks, T. A. Keith, M. J. Frisch, *J. Chem. Phys.* **1996**, *104*, 5497–5509.

[8] a) *Avogadro: an open-source molecular builder and visualization tool. Version 1.2.0.* http://avogadro.cc/; b) M. D. Hanwell, D. E. Curtis, D. C. Lonie, T. Vandermeersch, E. Zurek, G. R. Hutchison, *J. Cheminform* **2012**, *4*, 17.

[9] D. A. Leas, Y. Dong, J. L. Vennerstrom, D. E. Stack, *Org. Lett.* **2017**, *19*, 2518–2521.

[10] E. Demory, V. Blandin, J. Einhorn, P. Y. Chavant, *Org. Process Res. Dev.* **2011**, *15*, 710–716.

[11] a) J. F. Ambrose, L. L. Carpenter, R. F. Nelson, *J. Electrochem. Soc.* **1975**, *122*, 876–894; b) L. Wei, J. Li, K. Xue, S. Ye, H. Jiang, *New J. Chem.* **2019**, *43*, 16629–16638.